Stockholm University

Cosmic Molecules and Clusters

Knockout Driven Reactions

Naemi Florin

Doctoral Thesis in Physics at Stockholm University, Sweden 2024

Cosmic Molecules and Clusters

Knockout Driven Reactions

Naemi Florin

Academic dissertation for the Degree of Doctor of Philosophy in Physics at Stockholm University to be publicly defended on Tuesday 19 March 2024 at 13.00 in sal FB42, AlbaNova universitetscentrum, Roslagstullsbacken 21 and online via Zoom, public link is available at the department website.

Abstract

Fullerenes and PAHs (polycyclic aromatic hydrocarbons) are two families of carbon based molecules. These are both present in the interstellar medium, and are there believed to play important roles in various processes, including the formation of stars in the case of PAHs. This thesis presents studies on the structures and dynamics of fullerenes and PAHs and their weakly bound clusters, that all have relevance in an astrophysical context. Here, the focus is on knockout driven reactions in which a single atom is knocked out of a molecule or a molecular cluster as a result of Rutherford-like scattering processes. These are modelled by means of classical molecular dynamics simulations.

The first study investigates knockout processes where a C_{60} molecule is collided with helium atoms at 166 eV in the centre-of-mass-frame, similar to the velocities in interstellar shocks. Using a combination of experimental measurements and molecular dynamics simulations we find that highly reactive C_{59} fragments can be created sufficiently cold to stabilise and survive indefinitely inisolation.

Following the first study, we model the structures and stabilities of mixed clusters of C_{60} and $C_{24}H_{12}$ (coronene) molecules. We find that the two molecular species do not mix very well, but that they like to be in compact formations. For larger pure coronene clusters, we find that the most stable clusters contain two interacting stacks, forming a shape that looks similar to a “handshake”. These results are consistent with earlier modelling studies. Here, we show that such stacks also show up as subclusters in large mixed clusters.

Finally, we use the most stable clusters from the second study as targets in collisions with 3 keV argon atoms. We find that the simulated mass spectra strongly resemble the corresponding experimental ones. These show that many various forms of new molecular structures, both fragments and large new molecules, are being formed, as a result of the collisions. Here, the simulations give information on the reaction pathways and on the structures of these new species. There are also examples of hydrogenated, but otherwise intact, fullerene and coronene molecules being formed.

The mechanisms we have studied mimic inter- and circumstellar conditions where shockwaves and stellar winds drive particles (atoms and ions) at velocities similar to those studied here. The reactions covered in this work are thus likely to take place in such environments when carbon-based molecules and grains are energetically processed.

Keywords: *Clusters, Fullerenes, PAHs, Knockout.*

Stockholm 2024
http://urn.kb.se/resolve?urn=urn:nbn:se:su:diva-226018

ISBN 978-91-8014-657-9
ISBN 978-91-8014-658-6

Stockholm University

Department of Physics

Stockholm University, 106 91 Stockholm

COSMIC MOLECULES AND CLUSTERS

Naemi Florin

Stockholm
University

Cosmic Molecules and Clusters

Knockout Driven Reactions

Naemi Florin

ISBN print 978-91-8014-657-9
ISBN PDF 978-91-8014-658-6

Cover art by the author
Printed in Sweden by Universitetsservice US-AB, Stockholm 2024

In memory of
Ragnhild Söderbergh
and Gunnar Florin

Acknowledgements

I want to thank my supervisors, Henning Zettergren and Michael Gatchell, for making it possible for me to finish this thesis. I also want to thank all of my atomic friends and colleagues and everyone else who, in one way or another, have been important to me during these years. Thanks also, of course, to my near and dear for all the love.

Abstract

Fullerenes and PAHs (polycyclic aromatic hydrocarbons) are two families of carbon based molecules. These are both present in the interstellar medium, and are there believed to play important roles in various processes, including the formation of stars in the case of PAHs. This thesis presents studies on the structures and dynamics of fullerenes and PAHs and their weakly bound clusters, that all have relevance in an astrophysical context. Here, the focus is on knockout driven reactions in which a single atom is knocked out of a molecule or a molecular cluster as a result of Rutherford-like scattering processes. These are modelled by means of classical molecular dynamics simulations.

The first study investigates knockout processes where a C_{60} molecule is collided with helium atoms at 166 eV in the centre-of-mass-frame (90 km/s), similar to the velocities in interstellar shocks. Using a combination of experimental measurements and molecular dynamics simulations we find that highly reactive C_{59} fragments can be created sufficiently cold to stabilise and survive indefinitely in isolation.

Following the first study, we model the structures and stabilities of mixed clusters of C_{60} and $C_{24}H_{12}$ (coronene) molecules. We find that the two molecular species do not mix very well, but that they like to be in compact formations. For larger pure coronene clusters, we find that the most stable clusters contain two interacting stacks, forming a shape that looks similar to a "handshake". These results are consistent with earlier modelling studies. Here, we show that such stacks also show up as subclusters in large mixed clusters.

Finally, we use the most stable clusters from the second study as targets in collisions with 3 keV argon atoms. We find that the simulated mass spectra strongly resemble the corresponding experimental ones. These show that many various forms of new molecular structures, both fragments and large new molecules, are being formed, as a result of the collisions. Here, the

simulations give information on the reaction pathways and on the structures of these new species. There are also examples of hydrogenated, but otherwise intact, fullerene and coronene molecules being formed.

The mechanisms we have studied mimic inter- and circumstellar conditions where shockwaves and stellar winds drive particles (atoms and ions) at velocities similar to those studied here. The reactions covered in this work are thus likely to take place in such environments when carbon-based molecules and grains are energetically processed.

Sammanfattning

Fullerener och PAH-föreningar (polycykliska aromatiska kolväten) är två familjer med kolbaserade molekyler. De har båda upptäckts i interstellära miljöer, och tros spela viktiga roller i diverse processer, bland annat antas PAH-molekyler spela nyckelroller då stjärnor bildas. Den här avhandlingen presenterar studier av enskilda fullerener och PAH-molekyler och deras kluster, som alla är relevanta i en astrofysikalisk kontext. Här ligger fokus på kollisionsprocesser i vilka en ensam atom slås ut från en molekyl eller ett molekylärt kluster som följd av Rutherford-liknande spridningsprocesser. I dessa studier används klassiska molekyldynamiksimuleringar.

Den första studien undersöker processer där en C_{60}-jon kolliderar med heliumatomer vid typiska hastigheter hos partiklar i interstellära chockvågor. Genom att använda en kombination av experimentella mätningar och molekyldynamiksimuleringar ser vi att högreaktiva C_{59}-fragment kan skapas tillräckligt kalla för att stabiliseras och överleva i all evighet i isolerat tillstånd.

Som uppföljning till den första studien modellerar vi blandade kluster av av fulleren- (C_{60}) och PAH- ($C_{24}H_{12}$) molekyler. Vi ser att de två molekylära sorterna inte blandas särskilt väl, men att de föredrar att vara i kompakta formationer. För större, rena PAH-kluster ser vi att de som är mest stabila består av två molekylära staplar som formar vad som påminner om ett "handslag". Detta resultat stämmer väl överens med tidigare modelleringsstudier. Här visar vi att sådana staplar också förekommer i större blandade kluster.

Slutligen använder vi de mest stabila klustren från den andra studien som måltavlor i kollisioner med 3 keV argonatomer. Vi får masspektra från simuleringarna som överensstämmer väl med experimentella resultat. Dessa visar att många olika sorters nya molekylära strukturer skapas, både fragment och nya större molekyler, som följd av kollisionerna. Här ger simuleringarna information om reaktionsvägarna och om strukturerna hos dessa

nya molekyler. Det finns också exempel på hydrogenerade, men i övrigt intakta, fulleren- och PAH-molekyler som skapas.

Mekanismerna vi har studerat efterliknar inter- och cirkumstellära förhållanden där chockvågor och stjärnvindar driver partiklar (atomer och joner) i hastigheter liknande dem vi studerar här. När kolbaserade molekyler och stoftpartiklar kolliderar med sådana partiklar äger därför de reaktioner som studeras i det här arbetet sannolikt rum i sådana miljöer.

List of Papers

Paper I: **Stability of C_{59} Knockout Fragments from Femtoseconds to Infinity**
Michael Gatchell, Naemi Florin, Suvasthika Indrajith, José Eduardo Navarro Navarrete, Paul Martini, MingChao Ji, Peter Reinhed, Stefan Rosén, Ansgar Simonsson, Henrik Cederquist, Henning T. Schmidt and Henning Zettergren. Submitted.

Paper II: **Structures and stabilities of mixed clusters of fullerene and coronene molecules**
Naemi Florin, Henning Zettergren and Michael Gatchell. Submitted.

Paper III: **Bond breaking and making in mixed clusters of fullerene and coronene molecules induced by keV-ion impact**
Naemi Florin, Alicja Domaracka, Patrick Rousseau, Michael Gatchell and Henning Zettergren. Submitted.

Author's Contribution

In each of the three papers included in this thesis, I was responsible for developing and performing the molecular dynamics simulations, as well as analysing their output. As part of this, I wrote the software tools for generating input structures and for correctly sampling the parameter space involved in each study. I then performed the simulations using an open source and highly optimised software package as an integrator of the dynamics. To analyse the output from the simulations, I developed custom software tools to extract the relevant information for each study from the raw data. This included calculating energy distributions for the various products in the simulations, constructing tools to autonomously identify covalently bound products from a list of output atoms, and visualising the output of the analysis. My contributions to the three articles are briefly summarised here:

Paper I: **Stability of C_{59} Knockout Fragments from Femtoseconds to Infinity**
I performed all molecular dynamics (MD) simulations, analysed and interpreted the results and co-wrote the theoretical part of the manuscript.

Paper II: **Structures and stabilities of mixed clusters of fullerene and coronene molecules**
I co-planned and prepared the study, performed all MD simulations, analysed and interpreted the results and wrote the first full draft of the manuscript.

Paper III: **Bond breaking and making in mixed clusters of fullerene and coronene molecules induced by keV-ion impact**
I co-planned and prepared the study, performed all MD simulations, analysed and interpreted the results and co-wrote the manuscript.

Contents

Chapter 1

Introduction and Background

1.1 Fullerenes, PAHs and the Interstellar Medium

Carbon, the sixth chemical element in the period table, is – based on atomic weight – the fourth most abundant element in the universe, following hydrogen, helium and oxygen. [1] All known life on earth, as we know it, is carbon-based – about half of all biomass consists of carbon. This is due to its great ability to form stable bonds with a variety of different elements.

Some chemical elements can exist in multiple pure forms, referred to as allotropes, with the atoms bound together in different ways. The more famous of the carbonic allotropes forms are perhaps diamond, graphite and the single-layered graphene. If the carbon atoms form bonds to form a closed cage, with twelve pentagons and zero, two or more hexagons, the resulting molecule belongs to the allotrope called fullerene. The most famous fullerene is the so called Buckminsterfullerene, C_{60} – or buckyball, due to its football-like shape (see figure 1.1) – named after the architect Buckminster Fuller (the constructor of geodesic domes which resemble the molecule). C_{60}, the first fullerene ever identified, was discovered in the lab by Kroto *et al.* [2, 3] Some years later, as predicted by Kroto, the molecules were discovered to be present in the interstellar medium – in space. [4, 5]

Hydrocarbons are organic compounds built up by carbon and hydrogen atoms. One specific class of hydrocarbons is called polycyclic aromatic hydrocarbons (PAHs). Originally describing the fact that the molecules smell,

the aromaticity now refers to the property of having cyclic rings of atoms, with resonance structures having alternating single and double interatomic bonds. Aromatic molecules are typically planar, consist of hexagons and are stable. In practice, they are a piece of graphene with hydrogen atoms around the edges. That the molecules are polycyclic means that they consist of at least two such aromatic rings. Coronene is an example of a PAH with the chemical formula $C_{24}H_{12}$ and contains seven aromatic rings (to the right in figure 1.1). This class of molecules have long been known to exist in nature and have been extensively studied in the laboratory. [6–10] They have for instance been proposed as carriers of interstellar infrared emission bands since the early 1980s, [11–17] but only recently were the first individual PAH species actually discovered in the interstellar medium. [18, 19]

In addition to the interstellar picture, in a more down-to-earth scenario, both fullerenes and PAHs have turned out to be present and of great impact in combustion processes, like flames and the formation of soot. [20–23] PAHs are also widespread atmospheric air-pollutants, and make up a large part of the dangerous substances in tobacco smoke. [24] A larger exposure to such molecules might lead to e.g. lung cancer. [25–27]

In neither the case of fullerenes nor that of PAHs is it known whether their presence in the interstellar medium is a result of top-down processes (processes where the molecules are formed as a result of the disintegration of larger molecules), bottom-up processes (when the molecules are built up by smaller components), or both of these two. [28–35] Advancing the understanding of such processes is the main motivation for the research presented in this thesis.

1.2 Weakly Bound Clusters of Fullerenes and PAHs

Molecular clusters of fullerenes and PAHs are model systems for cosmic dust grains. [16, 36–38] Dust grains in astrophysical environments are believed to play a significant role in the formation of stars and planets, speeding up the creation of H_2 molecules, and are used in some models of star evolution. [39–41] Such a cluster is weekly bound by van der Waals or dispersion forces where the *intermolecular* bonds are typically much weaker than the *intramolecular* bonds. This means that if they are heated, the cluster will start to emit intact molecules rather than molecular fragments. The first experimental studies on fullerene clusters ($(C_{60})_N$) were carried out by Martin *et al* in 1993 (see figure 1.2) [42]. They showed that there are certain what

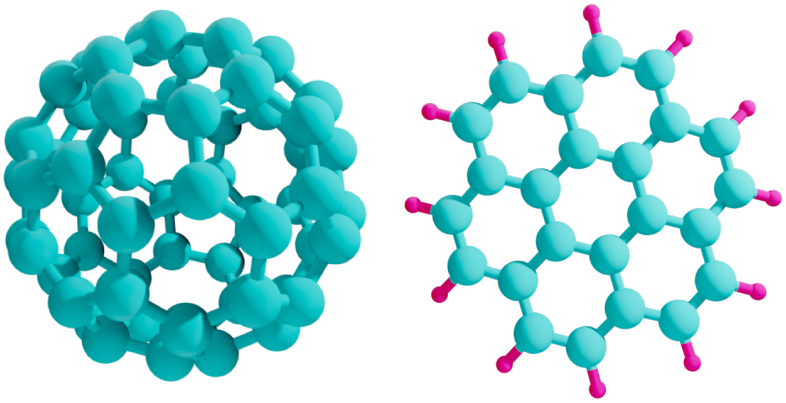

Figure 1.1: A fullerene, C_{60} (left) and a coronene, $C_{24}H_{12}$ (right) molecule.

they called "magic numbers" for which clusters of the corresponding sizes N are more stable and less likely to separate into individual molecules than their neighbouring sizes $N + 1$ and $N - 1$. Observations of magic numbers may then provide information about the packing type of the clusters. [43] For icosahedral clusters of packed spheres, one would expect to find magic numbers $N = 13$, 19 and 55 – which turned out to be exactly the numbers found in the study, as well as in later studies on the subject. [44–46] This stands in contrast to experimental studies on PAH clusters, for which no corresponding magic numbers have hitherto been found – likely due to high internal cluster excitation energies. [36, 47, 48]

Following these experimental findings, clusters of fullerene and PAH molecules have been studied theoretically and modelled, in order to further understand their formation processes, structures and stabilities. [43, 49–52] Among these many studies, $(C_{60})_N$ cluster formation was charted out in 1996 by Doye and Wales, for clusters of sizes up to $N = 80$ molecules. [53] They found, for example, that a cluster containing $N = 13$ molecules, shown in figure 1.3, is shaped like an icosahedron. This was a purely theoretical study where the authors used a Girifalco potential to model the intermolecular bonds. The Girifalco potential is specifically developed to be used with C_{60} molecules, and resembles a Lennard-Jones potential, but instead of explicitly treating the molecules as 60 discrete atoms, it approximates each molecule as a rotationally isotropic rigid sphere. [54]

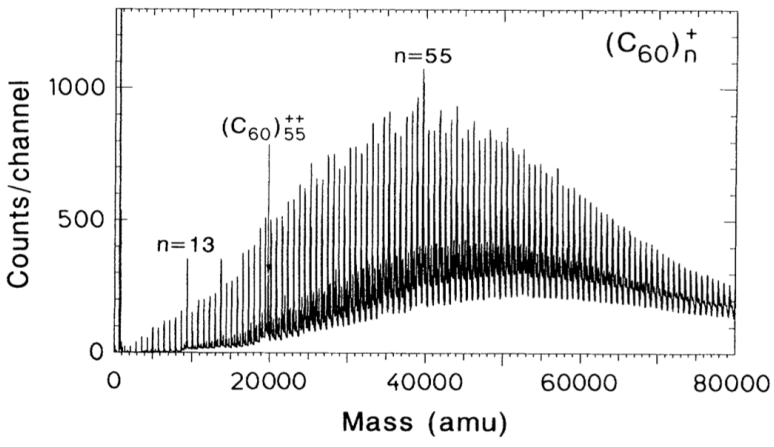

Figure 1.2: Mass spectrum for pure fullerene clusters of size n from the study by Martin *et al*, showing the magic numbers $n = 13$ and $n = 55$, corresponding to particularly stable clusters. (Note that while that study uses a lowercase n to denote cluster size, capital N is used for cluster size in our papers as well as in this thesis, and n the number of coronene molecules in the cluster). Reprinted figure with permission from T. P. Martin et al., Physical Review Letters, Vol 70, p. 3079-3082, 1993. Copyright 1993 by the American Physical Society.

In 2005, Rapacioli *et al.* theoretically investigated the cluster formation of pure clusters of PAHs – coronene molecules as well as other PAH species, with cluster sizes ranging from $N = 2$ to $N = 32$ molecules [55], using a combination of density functional theory (DFT) methods and Monte Carlo methods (basin-hopping and parallel tempering). They found that the lowest-energy structures, meaning the most stable structures, of PAHs are stacks – a single stack for clusters of up to $N = 8$ molecules. Clusters of $N = 9$ molecules and above form multiple stacks, that tend to combine into a so-called "handshake" structure, as shown in figure 1.4 for the case $N = 13$ (the figure is a part of the study further explained in paper II). The name refers to the two bent stacks meeting like two hands closing over each other. Larger clusters generally contain multiple smaller units (several small stacks and handshake structures), rather than two large stacks. [56] While their methods, unlike ours, take atomic and molecular charges into account, our results, as we shall see, agree very well with theirs.

1.3 Knockout Driven Reactions

1.3.1 Energy Transfer: Nuclear and Electronic Stopping

When colliding single ions with complex molecules and molecular clusters, a fraction of the kinetic energy of the projectile is in general transferred to the target. This is a type of process that may happen under controlled forms in the lab or in simulations, or naturally in, for example, the interstellar medium. [57,58] The transfer process itself can be the result of either electronic or nuclear stopping. [49,59]

Electronic stopping involves, as the name suggests, excitation of the electron cloud of the molecular or cluster target. [60,61] This is an inelastic process similar to friction, and it is the dominating source of energy absorption in the case of high-velocity collisions (velocities higher than a few hundred km/s). The electronic stopping power of a molecule can be defined as [62,63]

$$S = \frac{\mathrm{d}E}{\mathrm{d}R} = \gamma(r_s)v \tag{1.1}$$

where E is the projectile energy, R the distance from the target centre, γ the friction coefficient (also called density parameter) and v the projectile velocity. The friction coefficient – which, in a similar way as for a classical frictional force, governs the proportionality between velocity and stopping

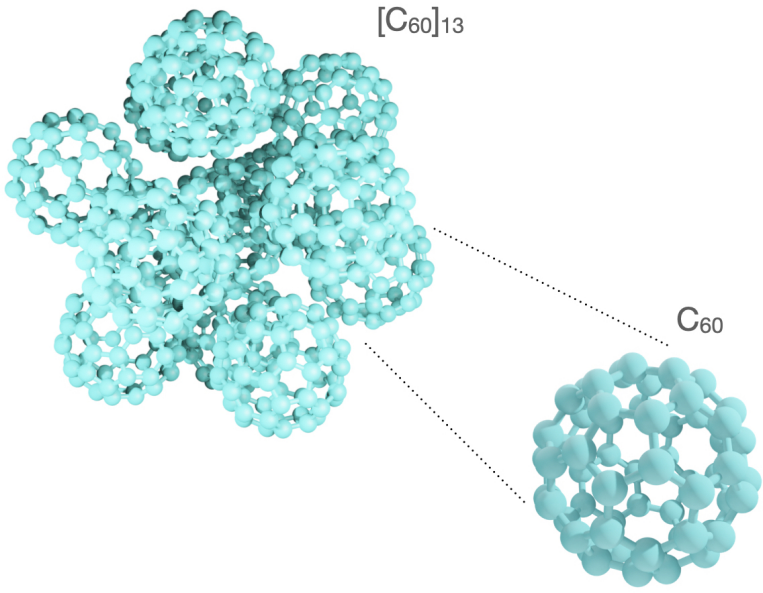

Figure 1.3: A $(C_{60})_N$ cluster of size $N = 13$ and a zoom-in of a single C_{60} molecule.

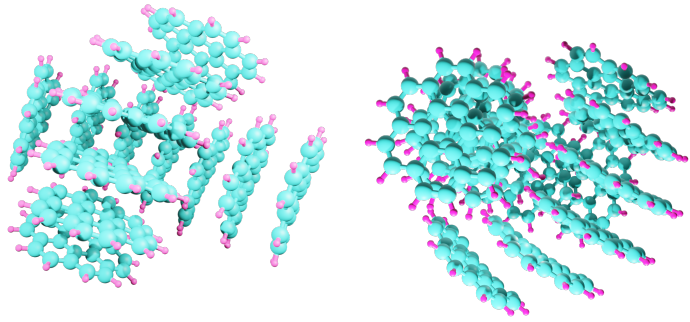

Figure 1.4: A pure coronene cluster of size $N = 13$, neatly forming the two-stack handshake structure, seen from two different angles.

power – depends on the free electron radius $r_s = \left(\frac{4}{3}\pi n_0\right)^{-\frac{1}{3}}$ (the electrons are described as a free electron gas), which in turn depends on the valence electron density n_0. The latter is specific for the target type – for instance, Puska and Nieminen modelled the valence electron density of a fullerene as a spherically symmetric jellium shell. [64] One may also use the electron density from quantum chemical calculations. [65]

Nuclear stopping, in turn, is when the projectile energy is transferred to the target nuclei in Rutherford-like scattering processes. Its theory was first developed based on work by Bohr. [66–69] It is basically an elastic process similar to hard spheres colliding with each other. This is the dominating energy transfer mechanism in low-velocity collisions (velocities up to a few hundred km/s) – that concerns all velocities relevant for the studies of this thesis. [70]

In its general form, nuclear stopping can be described via a screened Coulomb potential [70],

$$V(r) = \frac{Z_1 Z_2}{r} f(x) \tag{1.2}$$

where $Z_{1,2}$ are the charges of the target and the projectile, r the distance between the projectile and the target and $f(x)$ a screening function. The potential and screening function used in our studies is described in more detail in the next chapter.

In an elastic collision between a particle of kinetic energy E, mass M_1 and atomic number Z_1 collides with a second particle at rest (M_2, Z_2), the nuclear energy transfer to the second particle is then

$$T_{nuc} = T_{max} \sin^2\left(\frac{\phi}{2}\right). \tag{1.3}$$

where ϕ is the scattering angle in the centre-of-mass system and T_{max} the maximum energy transfer,

$$T_{max} = \frac{4 M_1 M_2}{(M_1 + M_2)^2} E. \tag{1.4}$$

The maximal energy transfer corresponds to a head-on collision between the projectile and the target.

1.3.2 Fragmentation Processes and Knockout Driven Reactions

After the energy transfer, an energetically excited molecule can further cool down and react in different ways, for example through statistical fragmentation (dominant on timescales up to milliseconds), non-statistical fragmentation (happens on femtosecond timescales) or photon emission (milliseconds and longer). Statistical fragmentation of molecules is a process where the excess energy activates dissociation channels after all the transferred energy has been spread out over the different molecular degrees of freedom. This is a process that happens on a timescale of picoseconds and longer. Another result of projectile energy absorption is the knockout of single atoms – a result of nuclear stopping that is unique to atom or ion collisions with molecules and cannot be the result of bombardment with electron or photon projectiles. This is a non-statistical fragmentation process since the energy is localised to the knocked out atom, rather than spread out over the molecule before the atom is released. There is a lower energy limit needed for the molecule to be able to release a single atom – the so called threshold displacement energy. This energy depends on the atom type and its bonds to its neighbouring atoms. Knockout molecular fragments are typically much more reactive than those produced in statistical fragmentation processes – this enables effective molecular growth in clusters that are hit by atomic or ionic projectiles. [49, 71]

The first findings of C_{59}^{+} ions as a result of a knockout process were performed in 1999 by Larsen *et al* – a study in which 50 keV C_{60} ions were collided with stationary gas targets of various gas types. [72] Many collision studies with C_{60} acting as a target have followed, with various ionic species used as projectiles. Collision simulations and experiments have also been performed with clusters as targets, both with pure C_{60} clusters, pure PAH clusters and with mixed clusters of C_{60} coronene molecules. [73, 74] These knockout experiments have given results in form of mass spectra of charged collision fragments. However, they do not give any insight into the detailed dynamics of the actual collision, or the survival of reaction products on short or long term timescales, only on the microsecond timescales relevant in the actual experiment. Here, theory and molecular dynamics simulations – methods that are further elaborated on in the next chapter – come into play. The molecular dynamics methods that we use in our simulations have been benchmarked in recent studies [75] and as we shall see, the mass spectra from our simulations agree very well with those from the corresponding experiments.

Altogether, all of these studies of cluster structures and cluster as well as single molecule collisions have acted as a background, inspiration and motivation for the thesis work. Our studies give further insights into the stability and longevity of knockout fragments of both single C_{60} molecules and molecular clusters of fullerenes and PAHs, presented in the first and third paper, respectively. To lay ground for the cluster knockout study, we performed the study on mixed cluster structures, presented in the second paper.

Chapter 2

Methods and Modelling

Before focusing on the specific studies of this thesis, this chapter aims to explain the general methods and models used to perform the simulations further described in the latter chapters.

2.1 Molecular Dynamics

Molecular dynamics (MD) is a collective name for different methods of calculating and simulating the behaviour and movement of atoms and molecules. In its purest form, MD uses Newton's second law ($F = ma$) to derive the trajectories of the particles involved, by numerically integrating said equation over time. [76]

Some MD methods, referred to as *ab initio* methods, or first principle methods, start by using the Born-Oppenheimer appromination, thus separating the motion of the electrons from those of the nuclei. One may then solve the Schrödinger equation for the electrons to get an effective nuclear potential energy, which is used to calculate the nuclear forces at that specific time step. This force calculation is then repeated for each timestep, and these forces are then used to derive the particle trajectories using Newton's equation of motion. In contrast to these *ab initio* methods, one can also use so called force field methods. In these, the potential function may or may not be derived from quantum mechanical first principles, but it is always an approximated model in which the potential surface has been parametrised. (A force field is the conventional name chemists and chemical physicists generally use for what other physicists would just refer to as the potential function). Classical molecular dynamics is a classical method based purely

on the integration of Newton's laws of motion. The software that we use in our simulations, LAMMPS (see section 2.2), uses classical force field methods to calculate the particle trajectories.

Ideally, one would intuitively choose *ab initio* models to perform all MD simulations since such methods start from an exact theory formulation. The main reason to why force field modelling is necessary is because ab initio computations quickly become too heavy for any computer to perform in a reasonable time. Nevertheless, given a well-constructed potential, the results from force field methods may very well be just as accurate as those from an *ab initio* dito. Force field MD methods have been successfully benchmarked and used in previous studies on fullerenes, PAHs and knockout processes. [71, 75, 77]

2.2 LAMMPS

LAMMPS – Large-scale Atomic/Molecular Massively Parallel Simulator – is an open-source classical molecular dynamics (MD) simulator, written in C++. [78,79] It was used to perform all simulations in this thesis. LAMMPS can be used entirely on its own but we used the LAMMPS Python interface in form of an imported Python module. This is key as it enabled the use of "regular" Python programming to prepare input and analyse output data, for example.

In LAMMPS, molecular simulations take place in a box of chosen size, whose edges can be set to be fixed, periodic or grow whenever a particle approaches its edges. Molecules are defined as a list of atomic ID:s, identifying the species of each atom, with three-dimensional coordinates for each atom. The bonds between the atoms are not defined per se, but the molecules are held together through classical force fields that are defined with chosen strengths and ranges. The systems are neutral, not modelling any electronic degrees of freedom. This is not a problem for the systems we are studying since both PAHs and fullerenes have a large number of electrons, making the bond strength practically unaltered by the removal or addition of an electron – previous similar studies have shown a good agreement between theory and experiment. [80] For the projectile velocities in our studies, nuclear stopping will be the dominant stopping force, hence making electronic stopping negligible. [49]

2.2.1 REBO

The REBO (Reactive Empirical Bond Order) potential, E^{REBO}, first proposed by Tersoff [81] and further developed into its present form by Brenner [82], is a short-ranged potential describing atomic and intramolecular interactions. Reactive means that the potential allows for bonds to break and for new bonds to form. It consists of a combination of a repulsive and an attractive term,

$$E_{ij}^{\mathrm{REBO}} = V_{ij}^{\mathrm{R}}(r_{ij}) + b_{ij}V_{ij}^{\mathrm{A}}(r_{ij}), \tag{2.1}$$

working pairwise on atoms i and j, distanced by r_{ij}. $b_{i,j}$ is a bond order between atoms i and j. Written out, the bond order actually contains a manybody-term, taking other neighbouring atoms into account. This allows for the bonds to dynamically change depending on the interaction between the atoms and their neighbours. REBO is defined solely with carbon and hydrogen atoms. It has been successfully used in previous studies of fullerenes [49], and was therefore our natural choice of molecular potential when studying single C_{60} molecules.

2.2.2 AIREBO

To model clusters of C_{60} and $C_{24}H_{12}$, we used an extension of the REBO potential called AIREBO (Adaptive Intermolecular Reactive Empirical Bond Order). Like REBO, it is defined to be used with carbon and hydrogen atoms. [82, 83] AIREBO is modelled as follows:

$$E = \frac{1}{2}\sum_{i}\sum_{j\neq i}\left[E_{ij}^{\mathrm{REBO}} + E_{ij}^{\mathrm{LJ}} + \sum_{k\neq i,j}\sum_{l\neq i,j,k} E_{kijl}^{\mathrm{TORSION}}\right], \tag{2.2}$$

summing over all pairwise interactions (ij), as well as taking interactions from the other atoms (k, l) into account. Here, E^{LJ} is a Lennard-Jones potential term which takes long-range interactions into account and E^{TORSION} is (as the name suggests) a torsional term. While the REBO term, as stated earlier, governs the atomic, intramolecular interactions, the LJ term models the intermolecular behaviour. It is the LJ term that is responsible for holding the clusters together. While REBO was a sufficient choice for our single-molecule collisions, we needed AIREBO and its LJ term for our cluster studies. AIREBO has previously been shown to well describe pure clusters of PAHs [71] and fullerenes [84] when bombarded with keV-atoms.

2.2.3 ZBL

For the atomic projectiles interacting with molecules and clusters, however, we needed a different kind of potential, both due to the different nature of the bond between two atoms in a molecule and that between a molecule and an external projectile, and because our chosen projectiles were neither carbonic nor hydrogenic. We chose the so-called ZBL (Ziegler-Biersack-Littmark) potential, which has been designed to describe high-energy atomic impact on solid targets. [85, 86] It is defined as:

$$E_{ij}^{ZBL} = \frac{1}{4\pi\epsilon_0}\frac{Z_i Z_j \mathrm{e}^2}{r_{ij}}\phi(r_{ij}/a) + S(r_{ij}), \tag{2.3}$$

where $a = 0.46850/(Z_i^{0.23} + Z_j^{0.23})$ and $\phi(x)$ is a sum of decreasing exponentials,

$$\begin{aligned}\phi(x) = 0.18175e^{-3.19980x} &+ 0.50986e^{-0.94229x} \\ &+ 0.28022e^{-0.40290x} + 0.02817e^{-0.20162x}.\end{aligned} \tag{2.4}$$

Here, ϵ_0 is the electrical permittivity of vacuum, $Z_{i,j}$ the nuclear charges of the atoms, e the elementary charge and r_{ij} the distance between the atoms i and j. $S(r)$ is a so called switching function, which decreases the potential value between an inner (r_1) and an outer (r_c) cutoff:

$$S(r) = C, \qquad r < r_1 \tag{2.5}$$

$$S(r) = \frac{A}{3}(r - r_1)^3 + \frac{B}{4}(r - r_1)^4 + C, \qquad r_1 < r < r_c \tag{2.6}$$

$$A = (-3E^{ZBL\prime}(r_c) + (r_c - r_1)E^{ZBL\prime\prime}(r_c))/(r_c - r_1)^2 \tag{2.7}$$

$$B = (2E^{ZBL\prime}(r_c) - (r_c - r_1)E^{ZBL\prime\prime}(r_c))/(r_c - r_1)^3 \tag{2.8}$$

$$C = -E^{ZBL}(r_c) + \frac{1}{2}(r_c - r_1)E^{ZBL\prime}(r_c) - \frac{1}{12}(r_c - r_1)^2 E^{ZBL\prime\prime}(r_c) \tag{2.9}$$

where $S'(r_1) = S''(r_1) = 0$, $S(r_c) = -E^{ZBL}(r_c)$, $S'(r_c) = -E^{ZBL\prime}(r_c)$ and $S''(r_c) = -E^{ZBL\prime\prime}(r_c)$. Here, the single and double primes mean first and second derivatives with respect to r. For small values of r_{ij}, the ZBL potential is simply an ordinary Coulomb potential. The so called screening function, $\phi(x)$, is an experimentally fitted function that determines the

behaviour of the potential at large distances. It simulates the screening effect of the electron cloud, which cuts off interactions between the atoms at larger interatomic distances. The total effect of this potential is the nuclear contribution to the stopping of the ionic projectiles when hitting its target atom or molecule, as well as the electronic screening. The latter is a purely static effect, dependent on the distance between the particles. In theory, there is also an electronic contribution to the stopping, as mentioned in the introduction. However, given the speed of the projectiles we are studying, the electronic contribution is negligible.

2.3 Setup

In all projectile-target simulations performed, it was necessary to ensure that the projectile hits from all possible directions, since the targets are not spherically symmetric. This could in principle be done by keeping the target positions fixed while completely randomising the projectile position. However, we found it simpler to equivalently limiting the projectile velocity to the z direction, and its initial position fixed and randomised in the xy-plane. When the target was a single C_{60} molecule, the target had a fixed centre of mass position and its initial coordinates were rotated by randomised angles. In the case of cluster targets, each molecule was randomly rotated around its own axis. Each molecule was randomly placed with its centre of mass at a set of pre-chosen coordinates that are fixed relative to each other but randomly rotated together as a cluster (more about the choice of coordinates in chapter 4).

To exclude projectile-target simulations where the projectile passes the target without transferring a non-negligible amount of energy – an exclusion mainly performed for time-economic purposes – we calculated the shortest projectile-target distance for which a negligible energy is transferred from the projectile to the target. This was done by isolating a single target atom of a specific kind, colliding it with the projectile of interest and manually fine-tuning the projectile starting position. In the actual simulations, the "unnecessary" simulations were then defined as those where the projectile-target distance just after optimisation were larger than said limit. The distance is easily calculated by projection of all atoms on the xy-plane (i.e. the plane orthogonal to the direction of the projectile). All simulations with distances larger than 3 Å (the energy transfer limit 2.78 Å, plus a small margin) were interrupted.

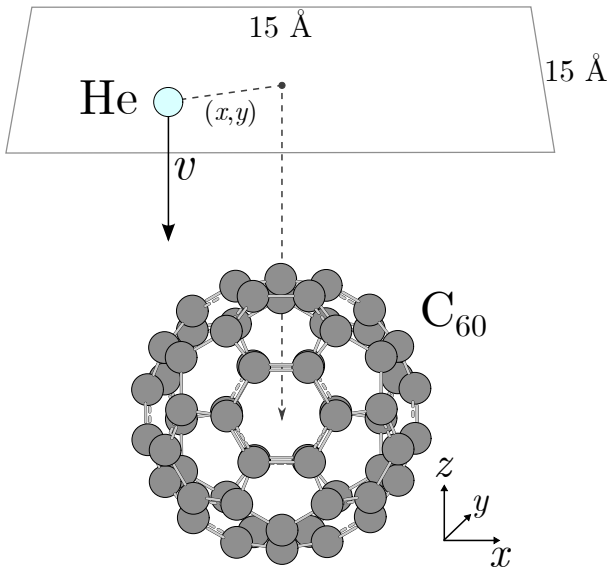

Figure 2.1: The simulation setup, with a helium atom acting as a projectile on a stationary C_{60} molecule.

2.4 Collision Output Analysis

The output data after a collisions is a set of atoms. Like the input data, each atom has an ID number and xyz-coordinates, as well as a velocity (v_x, v_y, v_z). Like the input file and all LAMMPS files, however, no interatomic bonds are defined. It is therefore not clear how to interpret the collision output, in terms of identifying the resulting atoms and molecules. We choose the interatomic distance 2 Å, long enough to cover both C-H (∼1 Å) and C-C (∼1.4 Å) bonds but shorter than van der Waals (∼3 Å) bonds, as the upper limit of what defines a molecular bond. A molecule is then defined as a set of atoms, all which are at such a distance or shorter to at least one other atom in the set.

For each collision, in the case of carbon atom knockout in single C_{60} collisions, the internal energy E_I of the C_{59} product was calculated,

$$E_I = E_{P,pre} - E_{P,post} - E_C - E_B - E_T \tag{2.10}$$

where $E_{P,pre}$, $E_{P,post}$ are the projectile energies pre and post collision, E_C is the energy of the single knocked out carbon atom and E_B the binding energy. E_T is the translational energy of the C_{59} product. The binding energy was calculated as the potential energy difference of single isolated C_{60} and C_{59} molecules. The internal energy of the C_{58} fragments were calculated in a similar fashion.

Chapter 3

Survival of Fullerene Knockout Fragments

The first study of this thesis, more thoroughly explained in paper I, investigates the occurrence of single atom knockout processes as a result of colliding atoms with C_{60} molecules. As we shall see, the presence of such knockouts were significant. The experiments in combination with the simulations showed that C_{59} anions are formed through knockout processes and they can remain stable on timescales of seconds and longer. Anions that have survived that long will no longer decay by emission of fragments but may cool radiatively – therefore they will survive indefinitely in isolation.

3.1 DESIREE Experiments

The collision and storage experiments were performed at the national research infrastructure DESIREE (Double ElectroStatic Ion Ring ExpEriment) at Stockholm University. [87] DESIREE is a cryogenic (13 K) ion-beam storage device, consisting of two large (8.7 m circumference) rings in which charged atoms and molecules can be stored. In our study of C_{59}^- fragments, stationary helium ions were bombarded with 30 keV C_{60}^- ions. This stands in contrast to our MD simulations, in which we, for practical reasons (it is easier to write the code for a stationary C_{60} and a single-atom projectile than the reverse situation), switched reference frames to that of the molecule and chose to bombard a stationary C_{60} molecules with a 167 eV He atom. Additionally, our simulations are, as previously mentioned, not

Figure 3.1: The DESIREE storage rings (see text).

taking any atomic or molecular charges into account, again in contrast to the charged real-life DESIREE experiments. Since DESIREE is only able to store charged particles, the collision output data will therefore only show the fraction of fragments that are charged. The MD simulations, in contrast, will show all neutral fragments, which is important to keep in mind when comparing the results from experiments and simulations, as we will show below.

The output that one can extract from such an experiment is measured in mass per charge, and the many collisions lead to a mass-per-charge spectrum with a more or less broad distribution of masses. Theoretically, the results are therefore not unambiguous, and in an experiment, one can never completely rule out the possibility of impurities. Nevertheless, the likelihood that helium atoms colliding with a C_{60} molecules or an impurity of the same mass yield something unexpected that shares the mass per charge of a C_{59} atom is negligible.

After yielding a mass spectrum, the fragments – C_{59} anions – are selected and stored in the storage rings for a longer period of time (up to 100 s), allowing for any spontaneous fragmentation to happen. The remaining C_{59} anions can then be counted, leading to an understanding of their survival on longer timescales. Two different types of measurements are made – the first one is spontaneous decay on short timescales up to milliseconds, where neutral particles are detected as a function of ion beam storage time. On longer timescales, no spontaneous decay is measured – there can however be remaining ions in the ring, that have cooled down enough to no longer decay. The remaining ions are therefore counted at different times by dumping them onto a detector, this way collecting data that can be turned into a decay curve for longer timescales. In total, it is observed that there are remaining ions after timescales of more than one minute, that are cold enough to not decay and that would remain intact indefinitely in isolation.

The more common C_{58} molecules that this experiment produces, however, can be produced either through a knockout process, or through statistical fragmentation (a dissociation process where a C_2 molecule is spontaneously emitted by a warm C_{60} molecule). The knockout can either be an immediate knockout of a C_2 molecule or two separate C atoms, or a two-step process, where a single carbon atoms is knocked out followed by emission of a second carbon atom (it takes about 4.5 eV for the C_{59} anion to lose a carbon atom). The dissociation process for statistical C_2 emission is far less frequent than knockouts, since the dissociation energy (about 10 eV) is much larger than the electron affinity of C_{60} (2.68 eV), making electron emission more likely than fragmentation. The large amount of C_{58}

molecules produced in the experiment are therefore expected to mainly be a result of knockout processes. C_2 dissociation, albeit unlikely, happens on the microsecond timescales involved in the DESIREE experiments. Here, our MD simulations are helpful. The simulations are performed on picosecond timescale processes, which allow us to extract the portion of the C_{58} production that is the result of a knockout, rather than of statistical fragmentation.

The long timescales on which the C_{59} fragments survive are illustrated in paper I, figure 5, where the number of surviving ions are plotted against time. This is the main result of this study – since a large fraction (15 %) of C_{59} ions survive on second timescales, timescales on which the ions do no longer decay, the general conclusion is that they survive indefinitely. But how can we understand that such a large amount survives knockout processes? Intuitively, head-on collisions with a single carbon knockout would lead to a large energy transfer, which in turn would make the C_{59} cage either fragment or emit an electron. Here, we are again helped by the MD simulations to understand what actually happens in the knockout processes on ultrashort timescales and to determine the internal energies of the knockout fragments.

3.2 MD Simulation Results

For the simulations corresponding to the DESIREE experiment, we used a cubic box with a side of 40 Å and shrink-wrapped, non-periodic edges. Shrink-wrapping refers to the property that a boundary expands if an atom approaches it, in order to keep all atoms contained within the box. As described in the previous chapter, a 167 eV helium projectile, launched in the z direction from a random xy-position on a 15 Å square, hit a stationary, randomly rotated C_{60} molecule.

The resulting internal energy distribution for the different species C_{60}, C_{59} and C_{58} are shown in paper I. As mentioned in the previous section, the reason for the large C_{58} peak is the combination of immediate C_2/2C knockout and single carbon knockout followed by emission of a second carbon atom. The corresponding MD peak only includes the former (knockout) processes. The energies are shown in the laboratory reference frame.

The internal energies of the respective molecular fragments are shown in paper I, figure 4. The higher amount of energy transferred to the fullerene "cage", the less likely is it to survive on long timescales. We see that C_{58} fragments in general are hotter, and therefore more likely to spontaneously decay further than C_{59} fragments. Such decay products are no longer pos-

sible to store in the ion rings.

The internal energy distribution also plays a crucial role when it comes to understanding the survival probability of the C_{59} anions. As mentioned earlier, 15 % of these anions produced in the experiments were shown to survive after a timescale of one minute. Although this is a large portion, it is significantly lower than the corresponding amount (80 %) of coronene fragments surviving a single carbon knockout. [77] A statistical analysis, however, explains this nicely. Using the Arrhenius rate equation, we calculated the maximal internal energy that a C_{59}^- can have to survive on the experimental timescales (for more details, see paper I). The MD internal energy analysis shows that only 20 % of the C_{59}^- fragments have internal energies below this threshold of 15 eV, which is consistent with the experimental results..

3.3 Discussion

An earlier knockout study, mentioned in the previous section and performed in DESIREE, investigated the knockout fragments of the PAH molecule coronene ($C_{24}H_{12}$). [77] These were also shown to survive indefinitely in the gas phase. There, it was discussed how interstellar shock waves affect PAH molecules – work previously done by Micelotta *et al.* [88] They showed that helium and hydrogen atoms collide with PAHs in shock waves of ≤ 75 km/s – such reactions correspond to the velocities of the projectiles used in the DESIREE study.

Coronene molecules are in general smaller than the typical PAHs found in space – however, secondary fragmentation will reduce with molecular size because of the increased number of degrees of freedom on which excess energy can be stored. Hence, the likelihood that interstellar PAHs will survive a knockout process increases with molecular size. It was thus motivated that similar results will be expected for large molecules such as fullerenes – something that the study of paper I confirmed.

Another interesting feature of the fragmentation are the new bonds that break and form in the defect molecules. Fullerenes and PAH molecules both consist of aromatic rings. However, while planar PAHs consist of six-atom rings, the fullerene is a combination of hexagons and pentagons. Knockout processes, however, can turn the hexagons of PAHs into pentagons, thus opening up for the possibility of bottom-up creation of fullerenes as a result of knockout. In the study of paper III, we will see that both fullerenes and PAHs also form heptagons and larger carbon rings as a result of knockout.

In a reverse process, we might therefore expect PAHs to be created as a top-down process from large hydrocarbon structures of the types formed in the experiments. The reactivity of a damaged PAH is also increased compared to an intact molecule – for instance the binding energy between an external H atom and a PAH molecule is increased by a factor of four after loss of a C atom, increasing the likelihood that new large molecules will be formed as a result of knockout. [70]

Similarly, C_{59} are also highly reactive molecules, and there are earlier studies showing how C_{58}^+ and C_{59}^+ ions react with C_{60} molecules, forming large "dumbbell" dimers. [89] However, this has previously only been shown to happen on short timescales. In space, the typical timescales between which atoms and molecules meet and are able to interact are long. Now that we know that C_{59} ions survive on long timescales on their own without decaying, we also know that the likelihood that they will meet other molecules to react with has increased significantly compared to if it only would have survived a short time after knockout. We learn more about what such reactions may look like in detail in paper III, which will be described further in chapter 4.

Chapter 4

Mixed Clusters of Fullerenes and PAHs: Structures and Knockout Reactions

The second part of this thesis, highlighting the results presented in papers II and III, concerns the stability of mixed clusters of fullerene and coronene molecules, and how these clusters behave when bombarded with single keV-ions. The MD results I present are compared to experimental results from the ARIBE facility in Caen that are first briefly described.

4.1 ARIBE/GANIL Experiments

ARIBE (Accélérateur pour la Recherche avec des Ions de Basse Energie, "accelerator for research with low energy ions") is a facility for low energy ion beam experiments located at the GANIL laboratory in Caen, France. Like our molecular dynamics simulations but in contrast to our previous C_{59} experiment in DESIREE, these specific experiments performed in ARIBE had stationary targets (fullerene/coronene clusters) with single ions used as projectiles in collision experiments. The projectiles were 22.5 keV He^{2+} and 3 keV Ar^{+} ions, respectively, in separate measurements. For 22.5 keV helium, the main stopping force is electronic stopping, while for 3 keV argon, nuclear stopping dominates.

The mixing ratio between the two molecular species could be adjusted in the experiments – mixing ratio in this case refers to the proportion between

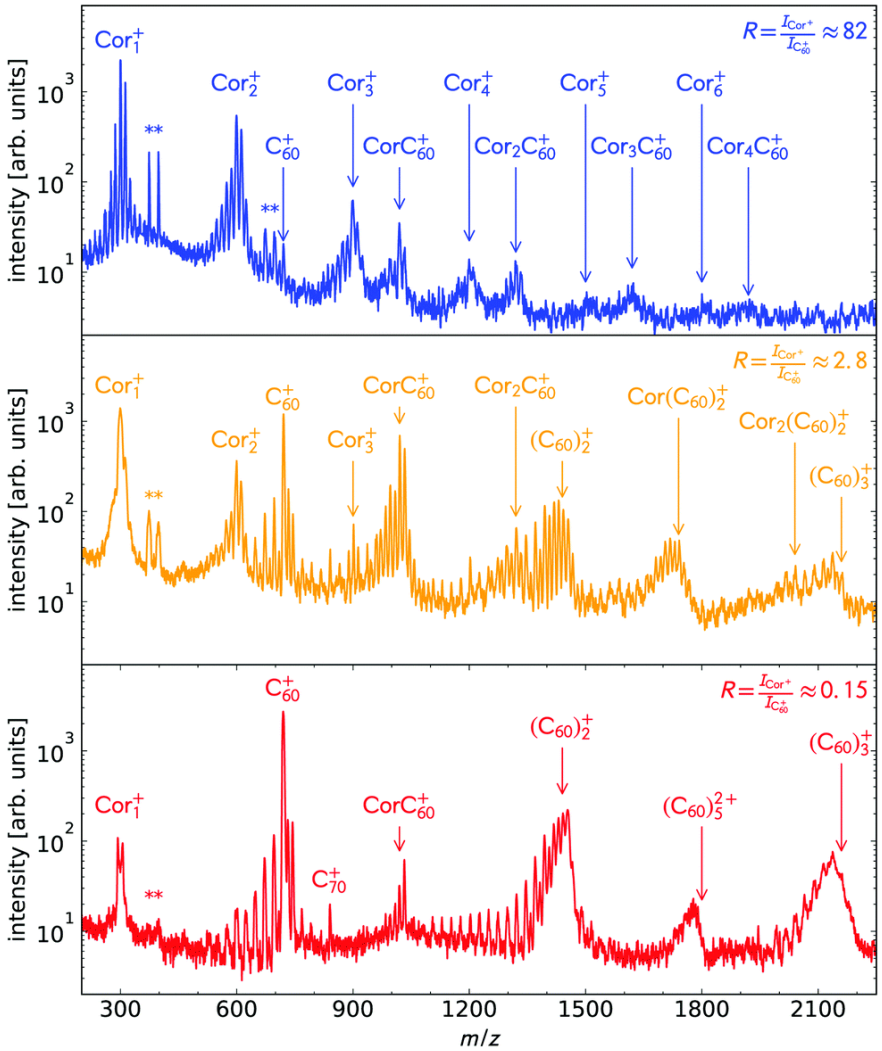

Figure 4.1: Mass spectra from a study of collisions between 3 keV Ar^+ and mixed clusters of coronene and fullerene molecules [74], with the different panels showing different mixing ratios (R) of coronene and fullerene molecules. The asterisks indicate impurities in the targets. Used with permission of Royal Society of Chemistry, from Ion collision-induced chemistry in pure and mixed loosely bound clusters of coronene and C_{60} molecules., A. Domaracka *et al*, vol. 20, issue 22, 2018; permission conveyed through Copyright Clearance Center, Inc.

the amount of coronene and C_{60} in the cluster aggregation source and hence reflect the typical mixing of these two species in the clusters. The ratios in the experiment were $R = I_{\mathrm{Cor}^+}/I_{\mathrm{C}_{60}^+} \approx 82$, 2.8 and 0.15, where I_{Cor^+} and $I_{\mathrm{C}_{60}^+}$ denote the intensities of coronene ($C_{24}H_{12}^+$) and C_{60}^+ cations respectively, meaning that one cluster distribution was dominated by coronene, one by C_{60} and one was a more equal mix of both species. The experiment yielded mass-per-charge (m/z) spectra, reflecting charge and energy transfer processes in the collisions. In contrast to the DESIREE experiments, however, these are so-called single-pass experiments, where the products ions are recorded on a microsecond timescale after the collision, without the ability of extracting any information on long-time decay dependencies.

Figure 4.1 shows the results of such an experiment for 3 keV Ar^+ impact performed by Domaracka et al [74], where nuclear stopping is dominant. The three mass–per-charge spectra show how the masses of the molecular fragments are distributed after collsions with clusters having three different mixing ratios (R), with markings for the masses of integer numbers of intact molecules, along with combinations of the two species. The upper panel corresponds to an almost pure coronene cluster. It shows that, apart from the peaks corresponding to masses of multiple coronene molecules, there are also peaks at the masses of various numbers of coronene molecules with a single C_{60} molecule attached. In the middle panel, with a larger fraction of C_{60} molecules than the first, shows peaks at various masses of mixed molecular products. Finally, in the third panel, whose target cluster consists mostly of C_{60} molecules, the main peaks correspond to the masses of integer numbers of intact C_{60} molecules. In between these large peaks are the smaller peaks of different reaction products, which are the most interesting part of the study, since they likely correspond to products of knockout processes, including e.g. hydrogenated and dehydrogenated molecules. These results do neither provide any information about the cluster structures nor the details of the collisions and how the molecules break and form new bonds. For this, we are, again, helped by MD simulations.

4.2 Cluster stabilities

Our initial reason to model mixed molecular clusters was to simulate cluster collisions, in the footsteps of Domaracka *et al.* [74] As a first step towards the collision simulations, we studied the stabilities of mixed clusters of various sizes and mixing ratios in order to gain more insight into their shapes, and to be able to choose the most stable structures as targets for the collisions.

This has previously been done by others for pure clusters of fullerenes and PAHs [53, 55], but never before for mixed clusters.

For clusters of N molecules with n coronenes and $N - n$ fullerenes, we chose the sizes $N = 5$ and $N = 13$. These numbers were chosen to be able to follow the mixing ratios in the experiments (see fig 4.1.), and also because $N = 13$ is a magic number in the case of pure C_{60} clusters. Here, magic number refers to the fact that the cluster forms a closed icosahedral shell for this specific number, as mentioned in the introduction and illustrated in figure 1.3. In addition, the relatively small cluster sizes gave us a reasonable time frame for the simulations – the experimental cluster distributions, in contrast, are likely also including larger ones. The reason for running two different sizes was to see if the results had a clear size dependence. For each cluster size N, we optimised the structures for all values of n ranging from $n = 0$ to $n = N$ – that is, we found energy minima on the potential surface, with the goal of finding the global minimum for each cluster (N, n). The simulations were run 10,000 times for each combination of N and n.

4.2.1 $N = 5$

For the smaller clusters, $(C_{24}H_{12})_n(C_{60})_{5-n}$, we found that the lowest energy structures are those containing stacked coronene molecules. There was a variation in cluster potential energy for the different values of n – the distributions are divided into peaks, with the number of peaks and the width of the distributions both increasing with increasing n, that is, with an increasing number of coronene molecules (see the full plot in paper II, figure 2). The peaks correspond to distinctive structure "families". Figure 4.2 shows typical structures from the different "families" for the case $n = 4$, below their corresponding potential energy spectrum. The lowest energy form is when all four coronene molecules are stacked in one stack with the fullerene at one end of the stack (family a). The next family in line is when the fullerene is placed next to the coronene stack, which then bends slightly to align with the curvature of the fullerene (family b). The two following families are quite similar, with a stack of three coronene molecules placed with the planar surface facing the fullerene (family c) or with the edges towards the fullerene (family d), both with the fourth coronene perpendicular to the stack. Next, the stack is reduced to two coronene molecules and the other two are bound to the fullerene from opposite sides, again perpendicular to the coronene stack (family e). The last family consists of a fullerene placed in the middle of four coronene molecules forming a square (family f). The maximal energy cluster of the same size and mixing ratio is also shown in

the figure.

4.2.2 $N = 13$

Compared to the case when $N = 5$, it is harder to define a general pattern when it comes to clusters of size $N = 13$, that is, $(C_{24}H_{12})_n(C_{60})_{13-n}$. In contrast to when $N = 5$, the clusters do not form distinct structure families, except perhaps in the case when $n = 13$ (pure coronene cluster). One can also see that, unlike the case when $N = 5$, the structure $n = 0$ has lower energy than the one where $n = 13$. This can be explained by the fact that the pairwise binding energy for the two molecular types are different, and it is easier for a fullerene to maximise the number of nearest neighbour interactions than it is for a coronene molecule. As Rapacioli *et al* showed [55], optimised pure PAH clusters start to form two separate stacks – the handshake structure – rather than a single one when $n = 8$ and larger, which we also see in our simulations. That our model gave that same shape for pure coronene clusters of size $N = 13$ (see figure 1.4) strongly supports our choice of model. For the mixed clusters, we see that the molecules tend to divide into "subclusters" consisting of one or multiple small coronene stacks and a separate number of fullerene molecules, when the number of coronene molecules is large enough (around $n = 6$). For a smaller number of coronene molecules, they tend to align with the surface of a centered fullerene subcluster. In general, the two molecular species do not mix very well.

4.3 Cluster collisions

With optimised cluster structures, we were now ready to perform the collision simulations briefly mentioned earlier in this chapter. Using a similar approach as in the study of He + C_{60} collisions, we bombarded four different cluster structures with 3 keV argon atoms. The clusters used as targets were the lowest energy structures for $N = 5$, $n = 1$ and $n = 3$, and $N = 13$, $n = 2$ and $n = 9$, that is, $(C_{24}H_{12})_1(C_{60})_4$, $(C_{24}H_{12})_3(C_{60})_2$, $(C_{24}H_{12})_2(C_{60})_{11}$ and $(C_{24}H_{12})_9(C_{60})_4$. We chose those specific clusters to approximately mimic the coronene/fullerene ratios $I_{Cor^+}/I_{C_{60}^+} = n/(N-n) = 2.8$ and 0.15 of the experimental study by Domaracka et al. [74]

In the present study, we focused on comparing the results of our collisions with those of the experimental study. Figure 4.3 shows mass spectra for clusters of sizes $N = 13$ and $N = 5$, as well as the corresponding experimental results previously shown in figure 4.1. The size limit of the smaller

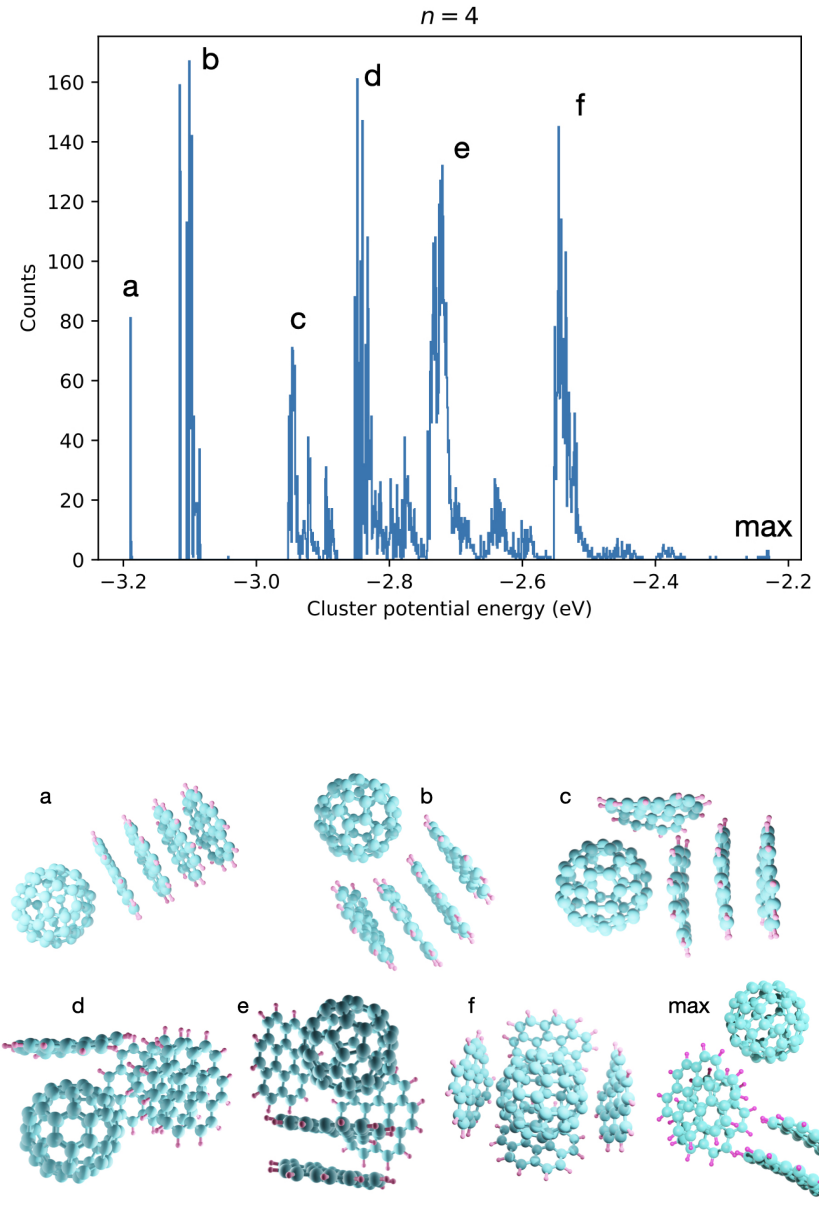

Figure 4.2: The upper panel shows the potential energy distribution for $(C_{24}H_{12})_4C_{60}$-clusters. The peaks labelled from a to f correspond to cluster "families" that have similar energies and hence structures. The energy of the most weakly bound cluster structure has the largest potential energy and is labelled "max". The lower panel shows representative clusters from the corresponding families.

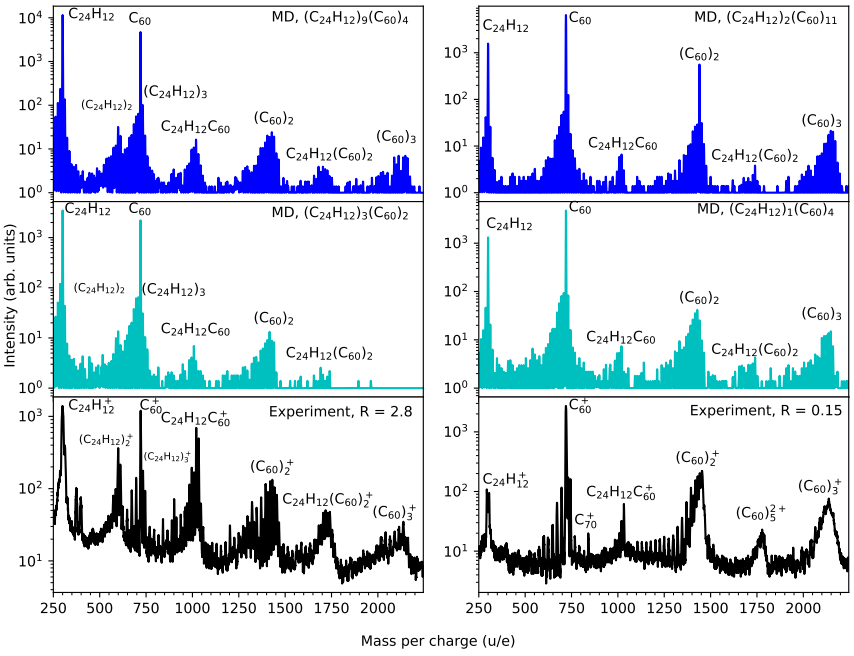

Figure 4.3: Mass spectra from collisions of 3 keV argon atoms with mixed clusters of fullerene and coronene molecules. Shown are the MD simulation results of cluster sizes $N = 13$ (top row) and $N = 5$ (middle row). The spectra in the left row are for clusters containing more coronene than fullerene molecules, while those in the right row are for clusters that predominantly contain fullerene molecules. The corresponding experimental results are shown in the lower row [74], for two different mixing ratios, $R = 2.8$ (left column) and $R = 0.15$ (right column).

clusters naturally leaves out the peaks for large masses for those clusters. However, for the smaller masses up to around $m = 1740$ u (which is the mass of one fullerene and two coronene molecules together), the results for the large and small clusters are strikingly similar, with only the intensities of different peaks varying with the number of available precursor molecules. In paper III, we therefore chose to only show the results for the larger clusters.

There, we also zoomed in on some specific fragment masses, corresponding to addition and subtraction of a carbon or a hydrogen atom from a fullerene-hydrogen dimer or a single molecule of either species ($m = 1008$ u, 1020 u and 1032 u), as well as some exotic cases. We found that most of such cases are a fullerene and a coronene bound together. This is not obvious since it takes more than 50 eV to push two intact, non-defect fullerenes together to form a covalently bound fullerene dimer [90] – this means they will only react with each other as a result of a knockout damage. However, since the mass is preserved, any knocked out atoms must have been picked up somewhere along the process. Another possible scenario is that the collision damaged at least one of the molecules without actually knocking out any atoms. We also found cases of pure carbonic molecules with the same mass as an intact mixed fullerene-coronene dimer (C_{85}), and with an additional (C_{86}) or a lost carbon atom (C_{84}). Furthermore, we found that it was common for hydrogen atoms to be bound to both coronene and fullerene molecules in other places than the regular coronene bonds, as a result of those hydrogen atoms being knocked out and absorbed by a neighbouring molecule – in such way creating new hydrogenated molecules. Such hydrogenated PAHs, for example, are believed to be an important contributor to H_2 formation in space. [91–93]

Here, I focus on masses around $m = 600$ u (two coronene) and $m = 1740$ u (one fullerene and two coronene). In figure 4.4, we see that it is indeed not only those molecular combinations yielding those masses. The figure shows some representative, interesting and varied cases of said masses. In both cases, fragmented fullerenes form more and less compactly bound purely carbonic molecules (a, g-i and l). There are also cases where one carbon atom is added to one of the coronene rings, forming a seven-atom-ring (f; $m = 612$ u), and we see that for masses around 1740 u, there are both cases where a coronene and a fullerene are both bound to a second fullerene (j, k, m), and where a coronene is sandwiched between two fullerenes (n). Some of the molecules are bound together through a single bond between two carbon atoms (b, e, j), while others form rings of three or more carbon atoms as the link between the molecules (c, k). There are also multiple examples of pure carbon molecules – most likely fragmented fullerenes – that have

formed both more compact structures (h, l) and structures with what looks like long carbonic tails (a, g, i). We additionally also here see examples of hydrogen atoms showing up in unexpected places, both on fullerenes, coronenes and mixes of the two species (k, n).

Most fragments of masses 600 u and 1740 u contain at least one coronene fragment. However, surprisingly many cases where said masses were found turned out to be purely carbonic molecules. In chapter 3, it was discussed how C_{59} knockout fragments might react with nearby molecules and form larger molecules. Here, we clearly see the result of such bottom-up reactions, that, as previously stated, are likely to happen in the interstellar medium due to the large survival probability of C_{59} shown in paper I. We also see examples of both increased and reduced numbers of carbon atoms in the carbon rings of both fullerene and coronene molecules, which speaks for the possibility of creation of one species from the other as a result of a top-down or bottom-up process respectively.

The molecular growth products shown in figure 4.4, however, are typically less stable compared to intact fullerenes and PAHs, and not formed in their ro-vibrational ground states.. They are hence likely to be further reduced by spontaneous decay on longer timescales than probed in the simulations, by energetic photons or electrons or by further knockout collisions with ions in stellar winds, that way creating somewhat smaller but more stable molecules. In such a way, the creation of new large molecules will be a combination of bottom-up and top-down processes simultaneously.

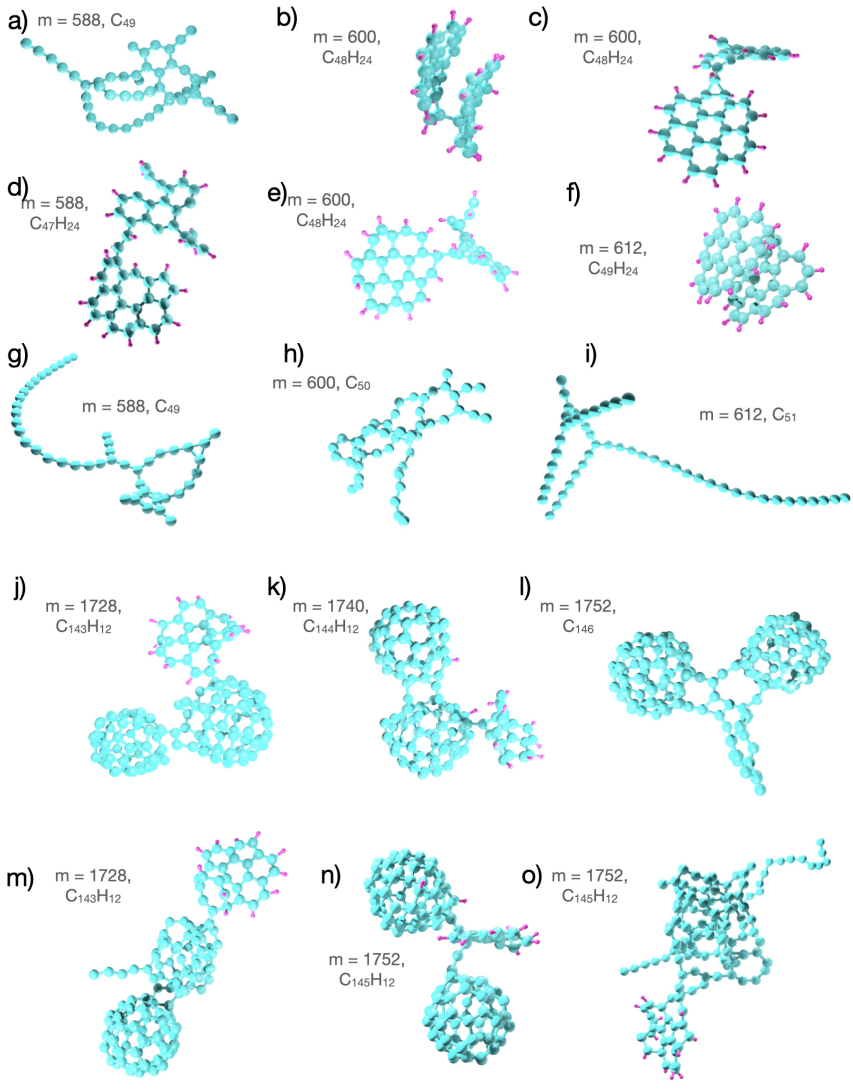

Figure 4.4: Examples of molecular growth products produced in collisions between 3 keV argon atoms and mixed clusters containing 9 coronene and 4 fullerene molecules. The growth products are all around the masses $m = 1740$ (corresponding to the mass of one coronene and two fullerene molecules) and $m = 600$ (corresponding to the mass of two coronene molecules).

Chapter 5

Conclusion and Outlook

The combination of direct, astronomical observations, of laboratory experiments and of MD simulation gives a deeper, richer understanding of the importance and role of molecular behaviour in the interstellar medium. Through studies of collisions with single C_{60} molecules as well as clusters of C_{60} and coronene molecules, we have come to a greater understanding of the structures of such clusters, of how the collision targets break and of how the fragments survive. These studies have advanced the understanding of knockout driven reactions, and pave the way for future studies in both molecular cluster physics and collision dito.

Earlier in this thesis, the understanding of top-down and bottom-up processes in context of the formation of molecules was presented as a key motivation for our work. We have seen examples of both such processes as a means of creation of new molecular species. In the first work on fullerene knockouts presented in this thesis, we showed that a significant portion of the C_{59} knockout fragments stabilise on millisecond timescales and thus survive indefinitely. Such fragments may thus exist in the interstellar environment, since similar knockout processes are there believed to occur in collisions between fullerenes and shock wave particles of the same velocities as our projectiles.

We next studied mixed clusters of fullerenes and coronenes, where we learned about the general structures that these form. This was important groundwork for our next study on cluster collisions, and since both fullerenes and coronene molecules are abundant in the interstellar environment, this study continues the work on interstellar molecules and how they interact and are processed there. We saw that the mixed clusters generally favoured being

separated into two pure subclusters. Concluding that study, we speculated that reaction products from the forthcoming collisions would also mainly being mixes of molecules of the same species. This turned out not to be the case.

Our third study on collisions between argon atoms and the clusters of our previous study showed that energetic atom impact leads to the build-up of new molecular species, dimers as well as larger structures, in accordance with the corresponding experimental study. [74] Like in the C_{59} knockout study, the argon projectiles may be used to mimic energetic particles in shock waves close to old stars, and the results are therefore believed to be relevant in better understanding interstellar environments. While argon has a low abundance in astrophysical processes, the fundamental processes studied here will be similar for any projectile atom. A similar study on that topic was done by Bernal *et al* [94], who collided 150 keV xenon atoms with a surface made of silicone carbide. This resulted in the creation of fullerenes, supporting the hypothesis that fullerenes may be created in space as a result of shock wave processing.

The study by Bernal and coworkers [94] paves the way for further work in the field. Given more time, we would have simulated such surface collisions to see if we would see any build-up of fullerenes, or if we would observe something completely different and unexpected. In general, the molecular dynamics simulation method is a very powerful tool that enables the understanding of molecular behaviour and processes on very short timescales, as well as the visualisation of atomic and molecular interactions – things that are often difficult to observe experimentally, as illustrated in this thesis. The good agreement between experiment and theory in cases where both are applicable support our choice of approach, and the simulations thereby provide us with valuable information that we might not have been able to find elsewhere.

Bibliography

[1] H. E. Suess and H. C. Urey, "Abundances of the elements," *Rev. Mod. Phys.*, vol. 28, pp. 53–74, Jan 1956.

[2] H. W. Kroto, H. W. Kroto, J. R. Heath, S. C. O'Brien, R. F. Curl, and R. E. Smalley, "C_{60}: Buckminsterfullerene," *Nature*, Nov 1985.

[3] H. Kroto, "Space, stars, C_{60}, and soot," *Science*, vol. 242, pp. 1139–1145, 2023/12/12 1988.

[4] J. Cami, J. Bernard-Salas, E. Peeters, and S. Malek, "Detection of C_{60} and C_{70} in a young planetary nebula," *Science*, vol. 329, pp. 1180–2, 09 2010.

[5] E. K. Campbell, M. Holz, D. Gerlich, and J. P. Maier, "Laboratory confirmation of C_{60}^+ as the carrier of two diffuse interstellar bands," *Nature*, vol. 523, pp. 322–323, July 2015.

[6] J. Szczepanski and M. Vala, "Infrared Frequencies and Intensities for Astrophysically Important Polycyclic Aromatic Hydrocarbon Cations," , vol. 414, p. 646, Sept. 1993.

[7] J. Banisaukas, J. Szczepanski, M. Vala, and S. Hirata, "Vibrational and electronic absorption spectroscopy of 2,3-benzofluorene and its cation," *The Journal of Physical Chemistry A*, vol. 108, no. 17, pp. 3713–3722, 2004.

[8] D. M. Hudgins, S. A. Sandford, and L. J. Allamandola, "Infrared spectroscopy of polycyclic aromatic hydrocarbon cations. 1. matrix-isolated naphthalene and perdeuterated naphthalene," *The Journal of Physical Chemistry*, vol. 98, no. 16, pp. 4243–4253, 1994. PMID: 12269375.

[9] D. M. Hudgins and L. J. Allamandola, "Infrared spectroscopy of matrix-isolated polycyclic aromatic hydrocarbon cations. 2. the members of the thermodynamically most favorable series through coronene," *The Journal of Physical Chemistry*, vol. 99, no. 10, pp. 3033–3046, 1995. PMID: 11538457.

[10] A. L. Mattioda, D. M. Hudgins, C. W. Bauschlicher, M. Rosi, and L. J. Allamandola, "Infrared spectroscopy of matrix-isolated polycyclic aromatic compounds and their ions. 6. polycyclic aromatic nitrogen heterocycles," *The Journal of Physical Chemistry A*, vol. 107, no. 10, pp. 1486–1498, 2003.

[11] A. G. G. M. Tielens, "Interstellar polycyclic aromatic hydrocarbon molecules," *Annual Review of Astronomy and Astrophysics*, vol. 46, no. 1, pp. 289–337, 2008.

[12] A. G. G. M. Tielens, "The molecular universe," *Reviews of Modern Physics*, vol. 85, pp. 1021–1081, 2013.

[13] A. Leger and J. L. Puget, "Identification of the 'unidentified' IR emission features of interstellar dust," *Astronomy and Astrophysics*, vol. 137, pp. L5–L8, 1984.

[14] K. Sellgren, "The near-infrared continuum emission of visual reflection nebulae," *The Astrophysical Journal*, vol. 277, pp. 623–633, 1984.

[15] A. Leger and L. B. D'Hendecourt, "The nature of very small grains: the PAH hypothesis.," in *Dust in the Universe* (M. E. Bailey and D. A. Williams, eds.), pp. 219–224, Jan. 1988.

[16] J. D. Bregman, L. J. Allamandola, A. G. G. M. Tielens, T. R. Geballe, and F. C. Witteborn, "The Infrared Emission Bands. II. A Spatial and Spectral Study of the Orion Bar," *The Astrophysical Journal*, vol. 344, p. 791, Sept. 1989.

[17] C. Joblin, A. Leger, and P. Martin, "Contribution of polycyclic aromatic hydrocarbon molecules to the interstellar extinction curve," *Astrophysical Journal Letters*, vol. 393, pp. L79–L82, 1992.

[18] B. A. McGuire, R. A. Loomis, A. M. Burkhardt, K. L. K. Lee, C. N. Shingledecker, S. B. Charnley, I. R. Cooke, M. A. Cordiner, E. Herbst, S. Kalenskii, M. A. Siebert, E. R. Willis, C. Xue, A. J. Remijan, and

M. C. McCarthy, "Detection of two interstellar polycyclic aromatic hydrocarbons via spectral matched filtering," *Science*, vol. 371, no. 6535, pp. 1265–1269, 2021.

[19] J. Cernicharo, M. Agúndez, C. Cabezas, B. Tercero, N. Marcelino, J. R. Pardo, and P. de Vicente, "Pure hydrocarbon cycles in tmc-1: Discovery of ethynyl cyclopropenylidene, cyclopentadiene, and indene," *A&A*, vol. 649, 2021.

[20] B. Haynes and H. Wagner, "Soot formation," *Progress in Energy and Combustion Science*, vol. 7, no. 4, pp. 229–273, 1981.

[21] H. Wagner, "Soot formation in combustion," *Symposium (International) on Combustion*, vol. 17, no. 1, pp. 3–19, 1979. Seventeenth Symposium (International) on Combustion.

[22] H. Richter and J. B. Howard, "Formation of polycyclic aromatic hydrocarbons and their growth to soot—a review of chemical reaction pathways," *Progress in Energy and Combustion Science*, vol. 26, no. 4–6, pp. 565–608, 2000.

[23] H. I. Abdel-Shafy and M. S. M. Mansour, "A review on polycyclic aromatic hydrocarbons: Source, environmental impact, effect on human health and remediation," *Egyptian Journal of Petroleum*, vol. 25, no. 1, pp. 107–123, 2016.

[24] S. S. Hecht, S. G. Carmella, S. E. Murphy, P. G. Foiles, and F.-L. Chung, "Carcinogen biomarkers related to smoking and upper aerodigestive tract cancer," *Journal of Cellular Biochemistry*, vol. 53, pp. 27–35, 2023/12/12 1993.

[25] X. Zhang, L. Zhang, L. Yang, Q. Zhou, W. Xing, A. Toriba, K. Hayakawa, Y. Wei, and N. Tang, "Characteristics of polycyclic aromatic hydrocarbons (pahs) and common air pollutants at wajima, a remote background site in japan," *International journal of environmental research and public health*, vol. 17, no. 3, p. 957.

[26] B. Moorthy, C. Chu, and D. Carlin, "Polycyclic aromatic hydrocarbons: from metabolism to lung cancer," *Toxicological sciences : an official journal of the Society of Toxicology*, vol. 145, no. 1, pp. 5–15, 2015.

[27] O. Viegas, I. Yebra-Pimentel, E. Martínez-Carballo, J. Simal-Gandara, and I. M. P. L. V. O. Ferreira, "Effect of beer marinades on formation of

polycyclic aromatic hydrocarbons in charcoal-grilled pork," *Journal of Agricultural and Food Chemistry*, vol. 62, no. 12, pp. 2638–2643, 2014. PMID: 24605876.

[28] H. Zettergren, H. A. B. Johansson, H. T. Schmidt, J. Jensen, P. Hvelplund, S. Tomita, Y. Wang, F. Martín, M. Alcamí, B. Manil, L. Maunoury, B. A. Huber, and H. Cederquist, "Magic and hot giant fullerenes formed inside ion irradiated weakly bound C_{60} clusters," *The Journal of Chemical Physics*, vol. 133, no. 10, p. 104301, 2010.

[29] J. Zhang, F. L. Bowles, D. W. Bearden, W. K. Ray, T. Fuhrer, Y. Ye, C. Dixon, K. Harich, R. F. Helm, M. M. Olmstead, A. L. Balch, and H. C. Dorn, "A missing link in the transformation from asymmetric to symmetric metallofullerene cages implies a top-down fullerene formation mechanism," *Nat Chem*, vol. 5, no. 10, pp. 880–885, 2013.

[30] L. Martínez, G. Santoro, P. Merino, M. Accolla, K. Lauwaet, J. Sobrado, H. Sabbah, R. J. Pelaez, V. J. Herrero, I. Tanarro, M. Agúndez, A. Martín-Jimenez, R. Otero, G. J. Ellis, C. Joblin, J. Cernicharo, and J. Martín-Gago, "Prevalence of non-aromatic carbonaceous molecules in the inner regions of circumstellar envelopes," *Nature Astronomy*, vol. 4, no. 1, pp. 97–105, 2020.

[31] Z. Meng and Z. Wang, "Evolution of fullerenes in circumstellar envelopes by carbon condensation: insights from reactive molecular dynamics simulations," *Monthly Notices of the Royal Astronomical Society*, vol. 526, pp. 3335–3341, 11/8/2023 2023.

[32] O. Berné and A. G. G. M. Tielens, "Formation of buckminsterfullerene (C_{60}) in interstellar space," *Proceedings of the National Academy of Sciences*, vol. 109, no. 2, pp. 401–406, 2012.

[33] J. Zhen, P. Castellanos, D. M. Paardekooper, H. Linnartz, and A. G. G. M. Tielens, "Laboratory formation of fullerenes from pahs: Top-down interstellar chemistry," *The Astrophysical Journal Letters*, vol. 797, no. 2, p. L30, 2014.

[34] O. Berné, J. Montillaud, and C. Joblin, "Top-down formation of fullerenes in the interstellar medium," *Astronomy and Astrophysics*, vol. 577, p. A133, 2015.

[35] V. J. Herrero, M. Jiménez-Redondo, R. J. Peláez, B. Maté, and I. Tanarro, "Structure and evolution of interstellar carbonaceous dust.

insights from the laboratory," *Frontiers in Astronomy and Space Sciences*, vol. 9, 2022.

[36] Ph. Bréchignac, M. Schmidt, A. Masson, T. Pino, P. Parneix, and C. Bréchignac, "Photoinduced products from cold coronene clusters," *Astronomy and Astrophysics*, vol. 442, no. 1, pp. 239–247, 2005.

[37] M. Rapacioli, C. Joblin, and P. Boissel, "Spectroscopy of polycyclic aromatic hydrocarbons and very small grains in photodissociation regions," *Astronomy and Astrophysics*, vol. 429, no. 1, pp. 193–204, 2005.

[38] M. Rapacioli, F. Calvo, C. Joblin, P. Parneix, D. Toublanc, and F. Spiegelman, "Formation and destruction of polycyclic aromatic hydrocarbon clusters in the interstellar medium," *A&A*, vol. 460, no. 2, pp. 519–531, 2006.

[39] J. L. Lemaire, G. Vidali, S. Baouche, M. Chehrouri, H. Chaabouni, and H. Mokrane, "Competing mechanisms of molecular hydrogen formation in conditions relevant to the interstellar medium," *The Astrophysical Journal Letters*, vol. 725, no. 2, p. L156, 2010.

[40] J. D. Thrower, L. Nilsson, B. Jørgensen, S. Baouche, R. Balog, A. C. Luntz, I. Stensgaard, E. Rauls, and L. Hornekær, "Superhydrogenated PAHs: Catalytic formation of H_2," in *EAS Publications Series* (C. Joblin & A. G. G. M. Tielens, ed.), vol. 46 of *EAS Publications Series*, pp. 453–460, 2011.

[41] J. D. Thrower, B. Jørgensen, E. E. Friis, S. Baouche, V. Mennella, A. C. Luntz, M. Andersen, B. Hammer, and L. Hornekær, "Experimental evidence for the formation of highly superhydrogenated polycyclic aromatic hydrocarbons through h atom addition and their catalytic role in H_2 formation," *The Astrophysical Journal*, vol. 752, no. 1, p. 3, 2012.

[42] T. P. Martin, U. Näher, H. Schaber, and U. Zimmermann, "Clusters of fullerene molecules," *Phys. Rev. Lett.*, vol. 70, pp. 3079–3082, May 1993.

[43] K. Hansen and H. Zettergren, "Clusters of fullerenes: Structures and dynamics," *The Journal of Physical Chemistry A*, vol. 126, no. 44, pp. 8173–8187, 2022. PMID: 36321908.

[44] K. Hansen, R. Müller, H. Hohmann, and E. E. B. Campbell, "Stability of clusters of fullerenes," *Zeitschrift für Physik D Atoms,Molecules and Clusters*, vol. 40, no. 1, pp. 361–364, 1997.

[45] W. Branz, N. Malinowski, H. Schaber, and T. P. Martin, "Thermally induced structural transition in $(C_{60})_n$ clusters," *Chemical Physics Letters*, vol. 328, no. 3, pp. 245–250, 2000.

[46] B. Manil, L. Maunoury, B. A. Huber, J. Jensen, H. T. Schmidt, H. Zettergren, H. Cederquist, S. Tomita, and P. Hvelplund, "Highly charged clusters of fullerenes: Charge mobility and appearance sizes," *Physical Review Letters*, vol. 91, p. 215504, 2003.

[47] A. I. S. Holm, H. Zettergren, H. A. B. Johansson, F. Seitz, S. Rosén, H. T. Schmidt, A. Ławicki, J. Rangama, P. Rousseau, M. Capron, R. Maisonny, L. Adoui, A. Méry, B. Manil, B. A. Huber, and H. Cederquist, "Ions colliding with cold polycyclic aromatic hydrocarbon clusters," *Physical Review Letters*, vol. 105, p. 213401, 2010.

[48] H. A. B. Johansson, H. Zettergren, A. I. S. Holm, F. Seitz, H. T. Schmidt, P. Rousseau, A. Ławicki, M. Capron, A. Domaracka, E. Lattouf, S. Maclot, R. Maisonny, B. Manil, J.-Y. Chesnel, L. Adoui, B. A. Huber, and H. Cederquist, "Ionization and fragmentation of polycyclic aromatic hydrocarbon clusters in collisions with keV ions," *Physical Review A*, vol. 84, p. 043201, 2011.

[49] M. Gatchell and H. Zettergren, "Knockout driven reactions in complex molecules and their clusters," *Journal of Physics B: Atomic, Molecular and Optical Physics*, vol. 49, p. 162001, aug 2016.

[50] H. A. B. Johansson, H. Zettergren, A. I. S. Holm, F. Seitz, H. T. Schmidt, P. Rousseau, A. Ławicki, M. Capron, A. Domaracka, E. Lattouf, S. Maclot, R. Maisonny, B. Manil, J.-Y. Chesnel, L. Adoui, B. A. Huber, and H. Cederquist, "Ionization and fragmentation of polycyclic aromatic hydrocarbon clusters in collisions with kev ions," *Phys. Rev. A*, vol. 84, p. 043201, Oct 2011.

[51] M. Nakamura and A. Ichimura, "Stability of multiply charged clusters of polycyclic aromatic hydrocarbons," *Physica Scripta*, vol. 2013, p. 014063, sep 2013.

[52] J. P. K. Doye, D. J. Wales, W. Branz, and F. Calvo, "Modeling the structure of clusters of C_{60} molecules," *Physical Review B*, vol. 64, pp. 235409–, 11 2001.

[53] J. P. Doye and D. J. Wales, "The structure of $(C_{60})_N$ clusters," *Chemical Physics Letters*, vol. 262, no. 1, pp. 167–174, 1996.

[54] L. A. Girifalco, "Molecular properties of fullerene in the gas and solid phases," *The Journal of Physical Chemistry*, vol. 96, no. 2, pp. 858–861, 1992.

[55] M. Rapacioli, F. Calvo, F. Spiegelman, C. Joblin, and D. J. Wales, "Stacked clusters of polycyclic aromatic hydrocarbon molecules," *The Journal of Physical Chemistry A*, vol. 109, no. 11, pp. 2487–2497, 2005. PMID: 16833550.

[56] M. Rapacioli and F. Spiegelman, "Modelling singly ionized coronene clusters," *The European Physical Journal D*, vol. 52, no. 1-3, pp. 55–58, 2009.

[57] E. R. Micelotta, A. P. Jones, and A. G. G. M. Tielens, "Polycyclic aromatic hydrocarbon processing in a hot gas," *Astronomy and Astrophysics*, vol. 510, p. A37, 2010.

[58] E. R. Micelotta, A. P. Jones, and A. G. G. M. Tielens, "Polycyclic aromatic hydrocarbon processing in interstellar shocks," *Astronomy and Astrophysics*, vol. 510, p. A36, 2010.

[59] J. Postma, S. Bari, R. Hoekstra, A. G. G. M. Tielens, and T. Schlathölter, "Ionization and fragmentation of anthracene upon interaction with keV protons and α particles," *The Astrophysical Journal*, vol. 708, no. 1, p. 435, 2010.

[60] Rosenblum, Salomon, "Recherches expérimentales sur le passage des rayons à travers la matière," *Ann. Phys.*, vol. 10, no. 10, pp. 408–471, 1928.

[61] H. Bethe, "Zur theorie des durchgangs schneller korpuskularstrahlen durch materie," *Annalen der Physik*, vol. 397, no. 3, pp. 325–400, 1930.

[62] J. Postma, S. Bari, R. Hoekstra, A. G. G. M. Tielens, and T. Schlathölter, "Ionization and fragmentation of anthracene upon interaction with keV protons and α particles," *The Astrophysical Journal*, vol. 708, p. 435, dec 2009.

[63] T. Schlathölter, O. Hadjar, R. Hoekstra, and R. Morgenstern, "Strong velocity effects in collisions of He^+ with fullerenes," *Phys. Rev. Lett.*, vol. 82, pp. 73–76, Jan 1999.

[64] M. J. Puska and R. M. Nieminen, "Photoabsorption of atoms inside C_{60}," *Phys. Rev. A*, vol. 47, pp. 1181–1186, Feb 1993.

[65] T. Chen, M. Gatchell, M. H. Stockett, J. D. Alexander, Y. Zhang, P. Rousseau, A. Domaracka, S. Maclot, R. Delaunay, L. Adoui, B. A. Huber, T. Schlathölter, H. T. Schmidt, H. Cederquist, and H. Zettergren, "Absolute fragmentation cross sections in atom-molecule collisions: Scaling laws for non-statistical fragmentation of polycyclic aromatic hydrocarbon molecules," *The Journal of Chemical Physics*, vol. 140, p. 224306, 06 2014.

[66] N. Bohr, "Ii. on the theory of the decrease of velocity of moving electrified particles on passing through matter," *The London, Edinburgh, and Dublin Philosophical Magazine and Journal of Science*, vol. 25, no. 145, pp. 10–31, 1913.

[67] N. Bohr, "Lx. on the decrease of velocity of swiftly moving electrified particles in passing through matter," *The London, Edinburgh, and Dublin Philosophical Magazine and Journal of Science*, vol. 30, no. 178, pp. 581–612, 1915.

[68] "Xxii. the penetration of atomic particles through matter," in *The Penetration of Charged Particles through Matter (1912–1954)* (J. Thorsen, ed.), vol. 8 of *Niels Bohr Collected Works*, pp. 423–568, Elsevier, 1987.

[69] J. Lindhard, M. Scharff, and H. E. Schioett, "Range concepts and heavy ion ranges (notes on atomic collisions, ii)," *Kgl. Danske Videnskab. Selskab. Mat. Fys. Medd.*

[70] T. Chen, M. Gatchell, M. H. Stockett, J. D. Alexander, Y. Zhang, P. Rousseau, A. Domaracka, S. Maclot, R. Delaunay, L. Adoui, B. A. Huber, T. Schlathölter, H. T. Schmidt, H. Cederquist, and H. Zettergren, "Absolute fragmentation cross sections in atom-molecule collisions: Scaling laws for non-statistical fragmentation of polycyclic aromatic hydrocarbon molecules," *The Journal of Chemical Physics*, vol. 140, p. 224306, 06 2014.

[71] R. Delaunay, M. Gatchell, P. Rousseau, A. Domaracka, S. Maclot, Y. Wang, M. H. Stockett, T. Chen, L. Adoui, M. Alcamí, F. Martín, H. Zettergren, H. Cederquist, and B. A. Huber, "Molecular growth inside of polycyclic aromatic hydrocarbon clusters induced by ion collisions," *The Journal of Physical Chemistry Letters*, vol. 6, no. 9, pp. 1536–1542, 2015. PMID: 26263308.

[72] M. Larsen, P. Hvelplund, M. Larsson, and H. Shen, "Fragmentation of fast positive and negative c ions in collisions with rare gas atoms," *The*

European Physical Journal D - Atomic, Molecular, Optical and Plasma Physics, vol. 1999, pp. 283–289, feb 1999.

[73] M. Gatchell, P. Rousseau, A. Domaracka, M. H. Stockett, T. Chen, H. T. Schmidt, J. Y. Chesnel, A. Méry, S. Maclot, L. Adoui, B. A. Huber, H. Zettergren, and H. Cederquist, "Ions colliding with mixed clusters of C_{60} and coronene: Fragmentation and bond formation," *Phys. Rev. A*, vol. 90, p. 022713, Aug 2014.

[74] A. Domaracka, R. Delaunay, A. Mika, M. Gatchell, H. Zettergren, H. Cederquist, P. Rousseau, and B. A. Huber, "Ion collision-induced chemistry in pure and mixed loosely bound clusters of coronene and C_{60} molecules," *Phys. Chem. Chem. Phys.*, vol. 20, pp. 15052–15060, 2018.

[75] M. H. Stockett, M. Gatchell, T. Chen, N. de Ruette, L. Giacomozzi, M. Wolf, H. T. Schmidt, H. Zettergren, and H. Cederquist, "Threshold energies for single-carbon knockout from polycyclic aromatic hydrocarbons," *The Journal of Physical Chemistry Letters*, vol. 6, no. 22, pp. 4504–4509, 2015. PMID: 26523738.

[76] M. Griebel, S. Knapek, and G. Zumbusch, "Numerical simulation in molecular dynamics, vol. 5 of texts in computational science and engineering," 2007.

[77] M. Gatchell, J. Ameixa, M. Ji, M. Stockett, A. Simonsson, S. Denifl, H. Cederquist, H. Schmidt, and H. Zettergren, "Survival of polycyclic aromatic hydrocarbon knockout fragments in the interstellar medium," *Nature Communications*, vol. 12, p. 6646, 2021.

[78] A. P. Thompson, H. M. Aktulga, R. Berger, D. S. Bolintineanu, W. M. Brown, P. S. Crozier, P. J. in 't Veld, A. Kohlmeyer, S. G. Moore, T. D. Nguyen, R. Shan, M. J. Stevens, J. Tranchida, C. Trott, and S. J. Plimpton, "Lammps - a flexible simulation tool for particle-based materials modeling at the atomic, meso, and continuum scales," *Computer Physics Communications*, vol. 271, p. 108171, 2022.

[79] "Lammps molecular dynamics simulator." https://lammps.sandia.gov.

[80] M. H. Stockett, M. Wolf, M. Gatchell, H. T. Schmidt, H. Zettergren, and H. Cederquist, "The threshold displacement energy of buckminsterfullerene C_{60} and formation of the endohedral defect fullerene $He@C_{59}$," *Carbon*, vol. 139, pp. 906–912, 2018.

[81] J. Tersoff, "New empirical approach for the structure and energy of covalent systems," *Phys. Rev. B*, vol. 37, pp. 6991–7000, Apr 1988.

[82] D. W. Brenner, O. A. Shenderova, J. A. Harrison, S. J. Stuart, B. Ni, and S. B. Sinnott, "A second-generation reactive empirical bond order (REBO) potential energy expression for hydrocarbons," *Journal of Physics: Condensed Matter*, vol. 14, p. 783, jan 2002.

[83] S. J. Stuart, A. B. Tutein, and J. A. Harrison, "A reactive potential for hydrocarbons with intermolecular interactions," *The Journal of chemical physics*, vol. 112, no. 14, pp. 6472–6486, 2000.

[84] R. Delaunay, M. Gatchell, A. Mika, A. Domaracka, L. Adoui, H. Zettergren, H. Cederquist, P. Rousseau, and B. Huber, "Shock-driven formation of covalently bound carbon nanoparticles from ion collisions with clusters of C_{60} fullerenes," *Carbon*, vol. 129, pp. 766–774, 2018.

[85] J. F. Ziegler and J. P. Biersack, *The Stopping and Range of Ions in Matter*, pp. 93–129. Boston, MA: Springer US, 1985.

[86] J. Ziegler, J. Biersack, and M. Ziegler, *SRIM, the Stopping and Range of Ions in Matter*. SRIM Company, 2008.

[87] H. T. Schmidt, R. D. Thomas, M. Gatchell, S. Rosén, P. Reinhed, P. Löfgren, L. Brännholm, M. Blom, M. Björkhage, E. Bäckström, J. D. Alexander, S. Leontein, D. Hanstorp, H. Zettergren, L. Liljeby, A. Källberg, A. Simonsson, F. Hellberg, S. Mannervik, M. Larsson, W. D. Geppert, K.-G. Rensfelt, H. Danared, A. Paál, M. Masuda, P. Halldén, G. Andler, M. H. Stockett, T. Chen, G. Källersjö, J. Weimer, K. Hansen, H. Hartman, and H. Cederquist, "First storage of ion beams in the double electrostatic ion-ring experiment: DESIREE," *Review of Scientific Instruments*, vol. 84, no. 5, p. 055115, 2013.

[88] Micelotta, E. R., Jones, A. P., and Tielens, A. G. G. M., "Polycyclic aromatic hydrocarbon processing in interstellar shocks," *AA*, vol. 510, p. A36, 2010.

[89] H. Zettergren, P. Rousseau, Y. Wang, F. Seitz, T. Chen, M. Gatchell, J. D. Alexander, M. H. Stockett, J. Rangama, J. Y. Chesnel, M. Capron, J. C. Poully, A. Domaracka, A. Méry, S. Maclot, H. T. Schmidt, L. Adoui, M. Alcamí, A. G. G. M. Tielens, F. Martín, B. A. Huber, and H. Cederquist, "Formations of dumbbell C_{118} and C_{119} inside clusters of C_{60} molecules by collision with α particles," *Physical Review Letters*, vol. 110, p. 185501, 2013.

[90] E. E. B. Campbell, *Fullerene-Fullerene Collisions*, pp. 161–189. Dordrecht: Springer Netherlands, 2003.

[91] C. Joblin, J. P. Maillard, I. Vauglin, C. Pech, and P. Boissel, "Probing the Connection between PAHs and Hydrogen (H, H_2) in the Laboratory and in the Interstellar Medium," in *Molecular Hydrogen in Space* (F. Combes and G. Pineau Des Forets, eds.), p. 107, Jan. 2000.

[92] Habart, E., Boulanger, F., Verstraete, L., Walmsley, C. M., and G. Pineau des Forêts, "Some empirical estimates of the H_2 formation rate in photon-dominated regions," *AA*, vol. 414, no. 2, pp. 531–544, 2004.

[93] Klærke, B., Toker, Y., Rahbek, D. B., Hornekær, L., and Andersen, L. H., "Formation and stability of hydrogenated pahs in the gas phase," *AA*, vol. 549, p. A84, 2013.

[94] J. J. Bernal, P. Haenecour, J. Howe, T. J. Zega, S. Amari, and L. M. Ziurys, "Formation of interstellar C_{60} from silicon carbide circumstellar grains," *The Astrophysical Journal Letters*, vol. 883, p. L43, oct 2019.